

Course LI, edited by M. S. Green (Academic, New York, 1971).

¹⁴D. P. Landau, *Phys. Lett.* **47A**, 41 (1974).

¹⁵E. Domany, K. K. Mon, G. V. Chester, and M. E. Fisher, *Phys. Rev. B* **12**, 5026 (1975).

¹⁶M. E. Fisher, in *Magnetism and Magnetic Materials*—

1974, edited by C. D. Graham, Jr., G. H. Lander, and J. J. Rhyne, AIP Conference Proceedings No. 24 (American Institute of Physics, New York, 1975), p. 273;

J. M. Kosterlitz, D. R. Nelson, and M. E. Fisher, *Phys. Rev. B* **13**, 412 (1976).

¹⁷K. Binder and D. P. Landau, *Surf. Sci.* **61**, 577 (1976).

Observation of the Two-Dimensional Plasmon in Silicon Inversion Layers

S. J. Allen, Jr., D. C. Tsui, and R. A. Logan

Bell Laboratories, Murray Hill, New Jersey 07974

(Received 18 March 1977)

The two-dimensional plasmon of an n inversion layer of (100) p -type Si is observed at a fixed wave vector as a function of electron density. The position, width, and strength of the resonance agree with existing theory at electron densities $\geq 10^{12}/\text{cm}^2$. At lower densities, the resonance position is below the predicted value, implying a substantial increase in the electron mass.

We have observed, in the far-infrared transmission through a silicon metal-oxide-semiconductor field-effect transistor (MOSFET), resonances which are due to plasmons in the two-dimensional (2D) electron gas that forms the inversion layer. The plasmons are coupled to the radiation field by locating a grating structure in proximity to the electron gas. At large inversion-layer electron densities, n_s , where the electron gas is metallic, the resonance position, width, and intensity agree in detail with a theory of the coupling of the plasmons and the radiation field, while at low densities, $< 10^{12}/\text{cm}^2$, difficulties are encountered that may be related to the anomalous electron localization often seen in these devices.

Plasma oscillations of a 2D electron gas differ in a nontrivial way from the corresponding oscillations in a 3D system. This difference stems from the fact that the restoring force for the charge-density oscillations for the 2D system is provided by the electrostatic field which remains 3D, fringing into the space on either side of the 2D sheet of charge. This has a number of important consequences that have been explored in great detail¹⁻¹³ from a theoretical point of view, beginning with the work of Ritchie¹ on thin metal foils. There are two key features. (1) The frequency of the 2D plasmon goes to zero as the wave vector goes to zero. (2) The frequency is perturbed by the shape and dielectric properties of matter in the immediate vicinity of the electron gas. In marked contrast to the extensive theoretical development, the only experiment that has directly probed the 2D plasmon is the work reported recently by Grimes and Adams¹⁴ and Platz-

man and Beni¹⁵ on electrons bound to a helium surface.

Our experiments were performed on an n -channel Si MOSFET with peak mobility of $16\,000\text{ cm}^2/\text{V sec}$ at 4.2°K . The device was fabricated on the (100) surface of a p -Si substrate with a net acceptor concentration $N_a - N_d = 1.1 \times 10^{15}\text{ cm}^{-3}$. The $1400\text{-}\text{\AA}$ dry gate oxide was grown at 1100°C . Fixed oxide charge $|Q_{ss}|$ was found to be $\leq 4 \times 10^{-10}\text{ cm}$. Interface state density was negligible, $< 1\%$ of the inversion-layer state density. The inversion layer was $250\text{ }\mu\text{m} \times 250\text{ }\mu\text{m}$ with conventional source and drain contacts. The gate electrode was a semitransparent Ti film (sheet resistance $\approx 350\text{ }\Omega/\text{sq}$), upon which was superimposed a grating of heavy gold metallization, with periodicity $a = 3.52\text{ }\mu\text{m}$ (see inset of Fig. 2). The dc device characteristics were unaltered by opening the transparent regions in the gold metallization. The electron density was obtained from the gate voltage, V_G , measured from the 77°K conduction threshold, V_T , and the oxide capacitance per unit area, C_{ox} , by $n_s = (C_{ox}/e)(V_G - V_T)$. Radiation was transmitted through the inversion layer, and the fractional change in transmission $\Delta T/T$, caused by introducing a fixed number of inversion-layer electrons, was measured with a conventional Fourier transform spectrometer.

In the absence of the grating, $-\Delta T/T$ measures directly the real conductivity, σ , of the space charge layer¹⁶

$$\text{Re}\sigma(\omega) \approx \frac{1}{2}(\Delta T/T)(Y_0 + Y_G + Y_S), \quad (1)$$

where Y_0 , Y_G , and Y_S are the wave admittances of free space, the metal gate, and the silicon sub-

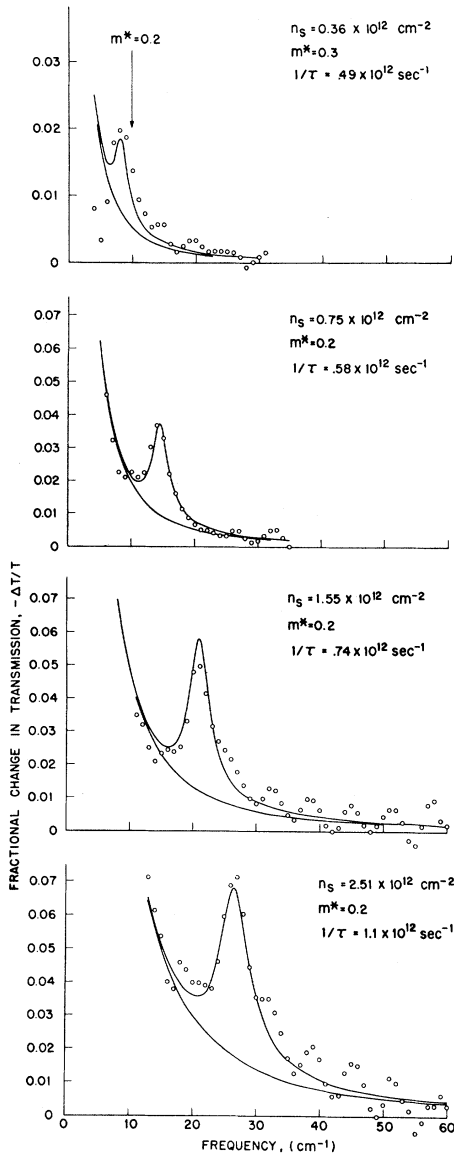


FIG. 1. Fractional change in transmission caused by inversion-layer electrons at 1.2°K. Resolution is 1 cm^{-1} . Solid curves are obtained from Eq. (3) with indicated mass and relaxation rate. The lower curve is the Drude part, the upper curve the full expression.

strate, respectively. The grating alters the wave admittance of the structure. For radiation polarized along the grating, it appears as a short circuit reflecting nearly all of the radiation. For radiation polarized perpendicular to it, the gate admittance Y_G has a capacitive component. Furthermore, in the near field of the grating, there is a longitudinal spatial modulation of the far-infrared field with the periodicity of the grating. This

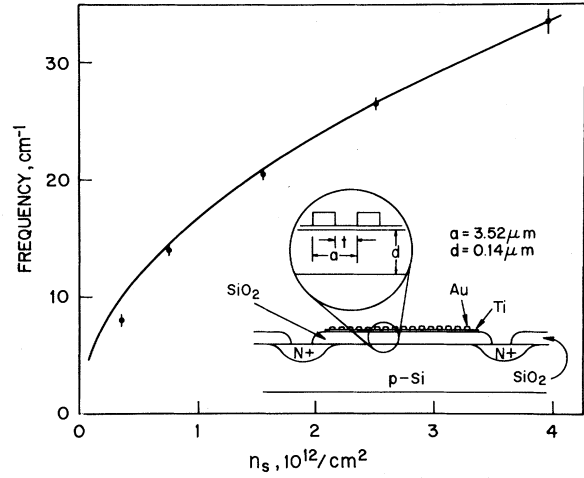


FIG. 2. Resonance position versus electron density, n_s . The solid curve is calculated from Eq. (2) using $m^* = 0.2$, $\epsilon_s = 12\epsilon_0$, and $\epsilon_{ox} = 4\epsilon_0$. Inset: cross section through Si MOSFET showing transparent gate and grating overlay, not to scale.

couples the radiation field to the plasma oscillations of the inversion layer electrons with wave vectors $q = n2\pi/a$ ($n = 1, 2, \dots$).

Figure 1 shows $-\Delta T/T$, as a function of frequency, for four different electron densities. Three features are evident: (1) absorption due to the Drude tail which couples to the spatially unmodulated part of the infrared field, (2) some oscillatory structure, especially apparent at large n_s , which is caused by interference in the Si substrate, and (3) a resonance peak which we identify as the 2D plasmon of the inversion layer at $q = 2\pi/a$.

Figure 2 shows the resonance position as a function of n_s . According to the theory developed by Nakayama¹¹ and Eguluz *et al.*,¹² the plasma frequency for the Si inversion layer at n_s is given by

$$\omega_p^2 = \frac{n_s e^2}{m^*} q \frac{1}{\epsilon_s + \epsilon_{ox} \coth(qd)}, \quad (2)$$

where m^* is the effective mass of the inversion layer electron, ϵ_s and ϵ_{ox} are the dielectric constants of Si and SiO_2 , respectively, and d is the oxide thickness. The solid curve is calculated from (2) using $m^* = 0.2$, $\epsilon_s = 12\epsilon_0$, and $\epsilon_{ox} = 4\epsilon_0$ together with $a = 3.52 \mu\text{m}$ and $d = 0.14 \mu\text{m}$ from our sample. It is seen that, except for the lowest density, there is good agreement between theory and experiment.

The fractional change in transmission through the structure is calculated explicitly in the limit

that the capacitive admittance of the grating is less than the effective dc sheet conductance of the metalization. We obtain

$$-\frac{\Delta T}{T} \times \frac{1}{2}(Y_0 + Y_G + Y_S) = \text{Re}\sigma(\omega) - \omega\epsilon_{\text{ox}}a \sum_{n=1}^{\infty} \frac{\sin^2(\pi n t/a)}{\pi^3 n^3} \left(\frac{Y_2 - Y_1}{(t/a)Y_2 + (1-t/a)Y_1} \right)^2 \text{Im} \left\{ \frac{[(\sigma/i\omega)(2\pi n/a) + \epsilon_s] \coth(2\pi n d/a) + \epsilon_{\text{ox}}}{(\sigma/i\omega)(2\pi n/a) + \epsilon_s + \epsilon_{\text{ox}} \coth(2\pi n d/a)} \right\}, \quad (3)$$

where Y_2 and Y_1 are the sheet conductances of the opaque and transparent regions, respectively, t is the width of open part of the grating, and $Y_G = Y_1 Y_2 / [(t/a)Y_2 + (1-t/a)Y_1]$. The zeros in the denominator of (3) give the plasmon dispersion relation derived by Nakayama¹¹ and Eguluz *et al.*¹²

The solid curves in Fig. 1 are obtained from (3) by keeping only the $n=1$ term. We assume that the gold is opaque, $Y_2 = \infty$, $Y_1^{-1} = 350 \Omega/\text{sq}$, and $t = 0.65a$.¹⁷ The only remaining adjustable parameters are the mass, m^* , and scattering rate, $1/\tau$. The background is clearly the Drude part, $\text{Re}\sigma(\omega)$, and the resonance the plasmon part. For electron densities above $10^{12}/\text{cm}^2$, we have taken the scattering rate derived from the dc conductivity, assuming a mass of 0.2. The fit leaves doubt that we are seeing the two-dimensional plasmon and that the coupling is properly given by (3). At the lowest two electron densities, the dc conductivity is thermally activated and we can no longer use the dc measurement to determine $1/\tau$. There we adjust m^* and $1/\tau$ for a best fit. More interesting, at $n_s = 0.36 \times 10^{12} \text{ cm}^{-2}$, the resonance position has shifted to frequencies below the prediction of (2). A fit to the resonance position can only be achieved if we assume that the mass has increased by a factor of 1.5 to 0.3 or n_s is reduced by ≈ 0.6 . We favor a mass increase. At present, there is considerable evidence that below $10^{12}/\text{cm}^2$ the electron mass is anomalous. We note the work of Kennedy *et al.*¹⁸ on the frequency dependence of the cyclotron mass for $n_s < 10^{12} \text{ cm}^{-2}$, and the work of Küblbeck and Kottbus¹⁹ and of Stallhoffer, Kottbus, and Koch²⁰ on stress- and temperature-dependent anomalies in the low-density mass. In fact, cyclotron resonance on devices from the same chip as the device described here has indicated a mass increase at low densities by as large as 1.5 in a magnetic field of 20 kG. It is not clear whether or not these mass shifts are related to the anomalous localization^{16,21,22} seen in this low-density limit.

It should be pointed out that the 2D behavior for the plasmon does not require that the electrons' motion be 2D at a microscopic level. It only re-

quires that the wavelength of the plasmon be large compared to the thickness of the slab of electrons.¹ This latter condition gives rise to two plasmon modes: one polarized normal to the slab, at the usual 3D plasma frequency,²³ and the other polarized along the slab, the 2D plasmons discussed here. For both the electrons on helium¹⁴ and the work described here, the quantum character of the motion normal to the surface which leads to microscopic 2D motion is incidental to the problem. In both cases, the wavelengths involved are sufficiently long that local expressions for the conductivity $\sigma(q=0, \omega)$ may be used. To extend the technique to large q vectors where interesting dispersion in σ is predicted appears difficult in the MOSFETs. As the periodicity is reduced, the oxide thickness must also be reduced; otherwise the coupling to the plasmon will become vanishingly small. Interesting effects in the dispersion of σ are not expected, however, until $q^{-1} \approx 100 \text{ \AA}$.^{6,7,10} Such a grating structure with equally small oxide thickness on large-area devices probably exceeds the capability of existing technology.

The plasmon probes $\sigma(q=0, \omega)$ of the inversion layer. It recovers in an unambiguous way both the real and the imaginary parts of σ . The resonance position determines the imaginary part, the width the real part of σ , and the effective mass is obtained in the absence of a magnetic field. Clearly, measurements in a magnetic field and searches for a low-frequency transverse plasmon,^{7,8} which can only exist in the presence of a highly correlated electron gas, may prove fruitful. The anomalous transport that is observed at $n_s < 10^{12} \text{ cm}^{-2}$ will also be further explored with the plasmon probe.

It is a pleasure to acknowledge the enlightening discussions with our colleagues G. A. Baraff, C. C. Grimes, R. D. Heidenreich, and P. M. Platzman. The technical assistance of F. DeRosa and G. Kaminsky is also appreciated.

¹R. H. Ritchie, Phys. Rev. **106**, 874 (1957).

²R. A. Ferrel, Phys. Rev. **111**, 1214 (1958).

- ³K. L. Kliever and R. Fuchs, Phys. Rev. **144**, 495 (1966), and Phys. Rev. **150**, 573 (1966).
⁴D. M. Newns, Phys. Rev. B **1**, 3304 (1970).
⁵N. J. Horing and M. Yildiz, Phys. Lett. **44A**, 386 (1973).
⁶F. Stern, Phys. Rev. Lett. **18**, 546 (1967).
⁷A. V. Chaplik, Zh. Eksp. Teor. Fiz. **62**, 746 (1972) [Sov. Phys. JETP **35**, 395 (1972)].
⁸R. S. Crandall, Phys. Rev. A **8**, 2136 (1973).
⁹A. L. Fetter, Ann. Phys. (N.Y.) **81**, 367 (1973).
¹⁰D. E. Beck and P. Kumar, Phys. Rev. B **13**, 2859 (1976).
¹¹M. Nakayama, J. Phys. Soc. Jpn. **36**, 393 (1974).
¹²A. Eguiluz, T. K. Lee, J. J. Quinn, and K. W. Chiu, Phys. Rev. B **11**, 4989 (1975).
¹³A. Caille and M. Banville, Solid State Commun. **19**, 951 (1976).
¹⁴C. C. Grimes and G. Adams, Phys. Rev. Lett. **36**, 145 (1976).
¹⁵P. M. Platzman and G. Beni, Phys. Rev. Lett. **36**, 626 (1976).
¹⁶S. J. Allen, Jr., D. C. Tsui, and F. DeRosa, Phys. Rev. Lett. **35**, 1359 (1975).
¹⁷ \hbar/a is measured to be ≈ 0.7 .
¹⁸T. A. Kennedy, R. J. Wagner, B. D. McCombe, and D. C. Tsui, to be published.
¹⁹H. Küblbeck and J. P. Kotthaus, Phys. Rev. Lett. **35**, 1019 (1975).
²⁰P. Stallhafer, J. P. Kotthaus, and J. F. Koch, Solid State Commun. **20**, 519 (1976).
²¹D. C. Tsui and S. J. Allen, Jr., Phys. Rev. Lett. **32**, 1200 (1974).
²²D. C. Tsui and S. J. Allen, Jr., Phys. Rev. Lett. **34**, 1293 (1975).
²³In the quantum 2D system, this plasma frequency becomes the plasma-shifted sub-band resonances; see, for example, S. J. Allen, Jr., D. C. Tsui, and B. Vinter, Solid State Commun. **20**, 425 (1976).

Spontaneous Relaxation of the Local 4f Magnetization in CePd₃†

E. Holland-Moritz, M. Loewenhaupt, and W. Schmatz

Institut für Festkörperforschung der Kernforschungsanstalt Jülich, 5170 Jülich, Germany

and

D. K. Wohlleben

II. Physikalisches Institut der Universität zu Köln, 5000 Köln 41, Germany

(Received 12 November 1976)

Diffuse neutron scattering on the intermediate valence compound CePd₃ shows a quasi-elastic line with Lorentzian shape and very large, nearly temperature-independent width ($\Gamma/2 \approx 20$ meV). The intensity under this line has 4f form factor but the total cross section indicates only 0.5 4f electron per formula unit. These observations are interpreted by spontaneous relaxation of the local 4f magnetization due to interconfiguration fluctuation between 4f¹ and 4f⁰.

In intermediate-valence (IV) rare earth (RE) compounds the incompletely filled 4f shell of a given lattice cell may be visualized to move in time back and forth between two configurations with integral occupation numbers n and $n-1$.¹ It is of central importance to learn more about the temporal motion of the local cells, or, equivalently, about the structure of the local energy spectrum on a scale of order $\Delta E \approx \hbar/\tau$. The most important question is whether successive transitions on a given cell are correlated in time or not. An uncorrelated motion (spontaneous transition) leads to a simple Lorentzian broadening of the configurational levels ($\Gamma/2 = \hbar/\tau$), while correlated motion, e.g., driven by a strong tendency to magnetic order via the Ruderman-Kittel-Kasuya-Yosida (RKKY) interaction, should give a more complicated spectrum with sharp lines as $T \rightarrow 0$.

The lack of structure in the temperature dependence of the macroscopic susceptibility of many IV compounds, especially the absence of magnetic order or crystal-field effects at low temperatures, suggests uncorrelated motion.²

So far local measurements have established only upper³ and lower^{4,5} limits to the configurational lifetimes (10^{-15} sec $< \tau < 10^{-11}$ sec). There are reasons to expect τ to lie in the range 10^{-12} – 10^{-13} sec for most IV compounds. Obviously, then, thermal neutrons will be a good tool to study the configurational motion on its own temporal as well as spatial scale, as they have been for dilute alloys in connection with the Kondo⁶ and spin-glass⁷ problems.

In this Letter we report the first direct measurement of the energy spectrum of the local magnetic moment in an IV compound. We have em-